Electronic Supplementary Material (ESI) for Materials Chemistry Frontiers.

Supplementary Information for

Aggregation-Enhanced Emission in Tetraphenylpyrazine-Based Luminogens: Theoretical Modulation and Experimental Validation

Guangshuai Gong,[a] Haozhong Wu,[b] Tian Zhang,*[a] Zhiming Wang,*[b] Xinjin Li[a] and Yujun Xie[c]

[a] School of Chemistry and Chemical Engineering, Shandong University of Technology, Zibo 255049, China. E-mail: tzhang@sdut.edu.cn

[b] AIE institute, State Key Laboratory of Luminescent Materials and Devices, Center for Aggregation-Induced Emission, Guangdong Provincial Key Laboratory of Luminescence from Molecular Aggregates (South China University of Technology), Guangzhou 510640, China. E-mail: wangzhiming@scut.edu.cn

[c] Institute of Molecular Aggregation Science, Tianjin University, Tianjin 300072, China.

1. Syntheses and characterizations

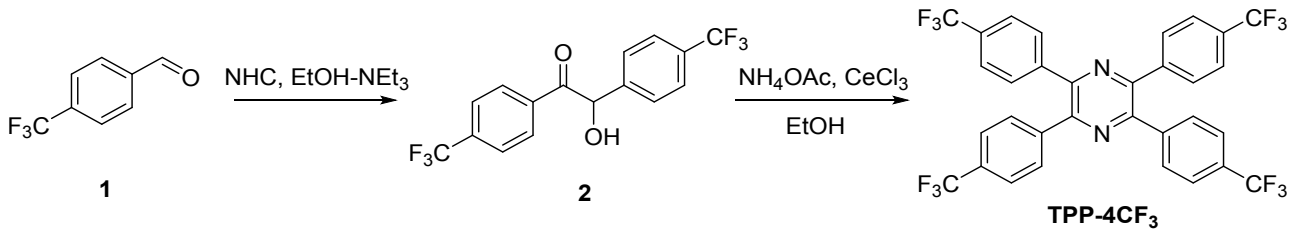

Chart S1 Synthetic routes to TPP-4CF_3.

2-hydroxy-1,2-bis(4-(trifluoromethyl)phenyl)ethan-1-one (**2**): 4-(trifluoromethyl)benzaldehyde **1** (40 mmol, 6.94 g) and NHC (3-benzyl-4-methyl-5-(2-hydroxyethyl)thiazole-3-ium·chloride) (4 mmol, 1.08 g) were added into two-neck bottle under nitrogen. After then, a mixed solvent system of triethylamine (1.65 mL, 12 mmol) and ethanol (32 mL) was injected into the bottle and the mixture was refluxed overnight under nitrogen atmosphere. After cooling to room temperature, the mixture was poured into water and extracted with dichloromethane three times and the combined organic layers were washed with brine, and then dried over $MgSO_4$. The solvent was removed under reduced pressure and the crude product was purified by column chromatography. White powder was obtained in the yield of 80%. ^{1}H NMR (500 MHz, CD_2Cl_2) δ 8.01 (d, J = 8.2 Hz, 2H), 7.70 (d, J = 8.3 Hz, 2H), 7.61 (d, J = 8.1 Hz, 2H), 7.48 (d, J = 8.1 Hz, 2H), 6.06 (s, 1H), 4.60 (s, 1H) ppm. ^{13}C NMR (126 MHz, CD_2Cl_2) δ 197.2, 141.5, 135.4, 134.2 (q, $J_{C\text{-}F}$ = 24.9 Hz), 129.8 (q, $J_{C\text{-}F}$ = 26.0 Hz), 128.6, 127.4. 125.4 (q, $J_{C\text{-}F}$ = 2.9 Hz), 125.1 (q, $J_{C\text{-}F}$ = 2.9 Hz), 123.1 (q, $J_{C\text{-}F}$ = 216.3 Hz) 122.6 (q, $J_{C\text{-}F}$ = 217.5 Hz), 75.2 ppm.

2,3,5,6-tetrakis(4-(trifluoromethyl)phenyl)pyrazine (**TPP-4CF_3**): **2** (3.48 g, 10 mmol), $CeCl_3$ $7H_2O$ (0.37 g, 1 mmol) and NH_4OAc (1.77 g, 23 mmol) were dissolved in ethanol (25 mL) at two-neck bottle and the mixture was stirring at 80 °C for 4 h. After cooling to room temperature, the mixture was poured into water and extracted with dichloromethane three times and the combined organic layers were washed with brine, and then dried over $MgSO_4$. The solvent was removed under reduced pressure and the crude product was purified by column chromatography. Yellow powder was obtained in the yield of 58%. ^{1}H NMR (500 MHz, CD_2Cl_2) δ 7.77 (d, J = 8.1 Hz, 8H), 7.65 (d, J =

8.2 Hz, 8H) ppm. ^{13}C NMR (126 MHz, CD_2Cl_2) δ 147.3, 140.4, 130.2 (q, $J_{C\text{-}F}$ = 32.8 Hz), 129.5, 124.7 (q, $J_{C\text{-}F}$ = 3.8 Hz), 123.3 (q, $J_{C\text{-}F}$ = 273.4 Hz) ppm.

2. ESP Explanations

In PRZ, average ESP value of carbon atoms in the pyrazine core is –0.56 (–0.10) kcal/mol in solid (solution). In TPP, those values in the pyrazine core and phenyl rings are −5.37 (−5.74) kcal/mol and −15.70 (−14.65) kcal/mol in solid (solution), respectively. The more negative ESP values in the pyrazine core for TPP compared to PRZ imply that the electron-rich phenyl rings introduce electronic conjugated effect to the electron-deficient pyrazine core. In TPP-4CF_3, above values are 11.29 (13.46) kcal/mol and 0.85 (2.80) kcal/mol in solid (solution). These results indicate that addition of the electron-withdrawing CF_3 groups to TPP peripheries can nearly equally increase the ESP values of the pyrazine core and phenyl rings by ~17 kcal/mol, but the difference between phenyls and pyrazine is still ~10 kcal/mol. The electronic conjugated effect of phenyls to pyrazine is not modified. Substitution with electron-donating OCH_3 groups can respectively decrease the ESP values of pyrazine and phenyls to −12.28 (−14.78) kcal/mol and −17.49 (−17.02) kcal/mol in solid (solution), which demonstrates increased electron density of the whole TPP skeleton and superior electronic conjugation merit of TPP-4OCH_3 to the others.

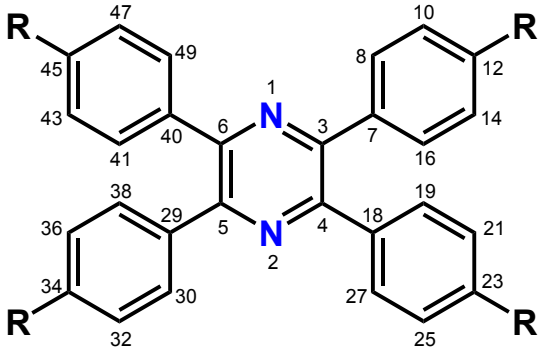

TPP **R = H**
TPP-4CF_3 **R = CF_3**
TPP-4OCH_3 **R = OCH_3**

Chart S2 Molecular structures of TPP and its derivatives with the labeled atom index.

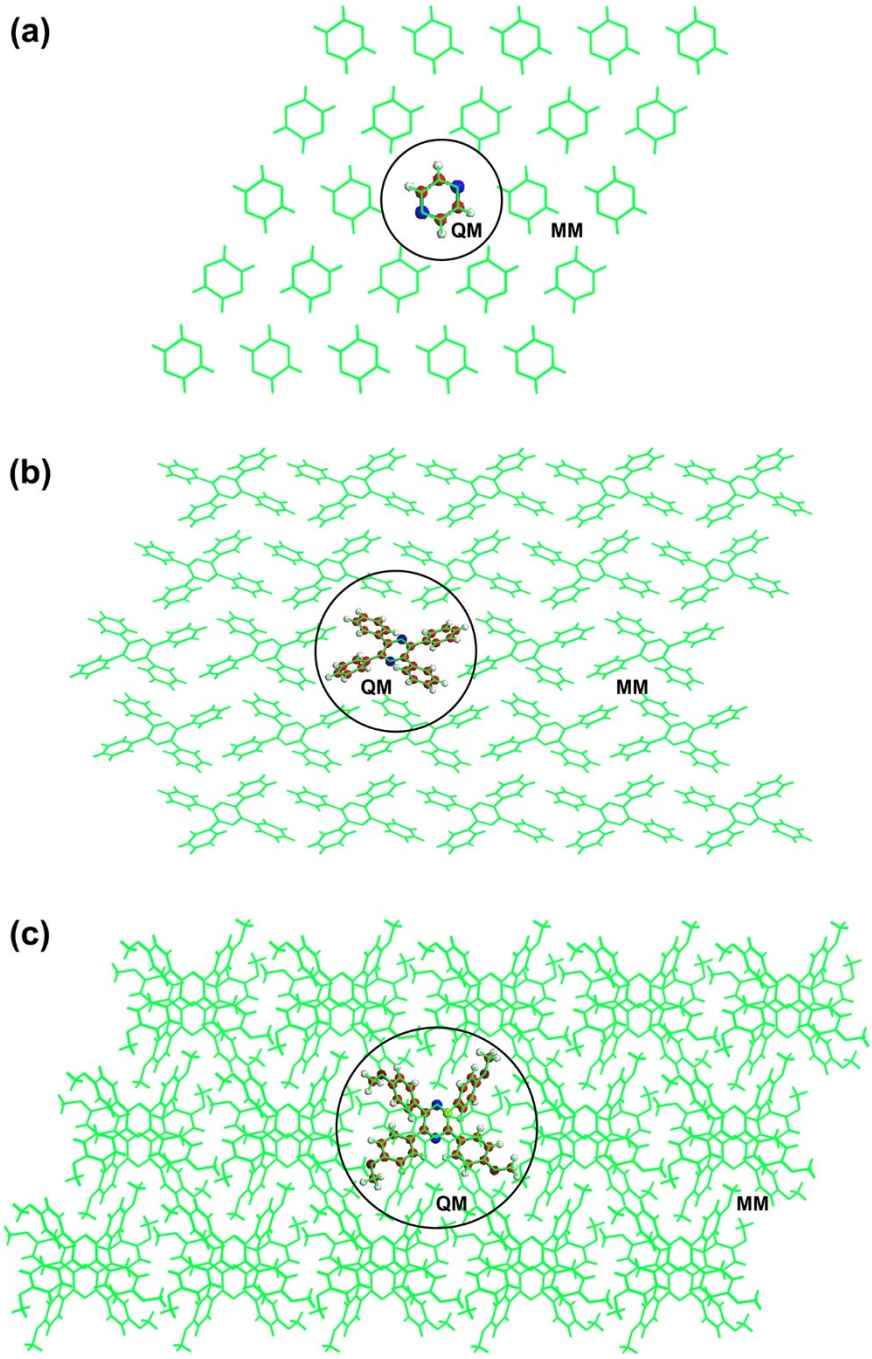

Fig. S1 Setup of the QM/MM models for PRZ (a), TPP (b) and TPP-4OCH_3 (c), respectively.

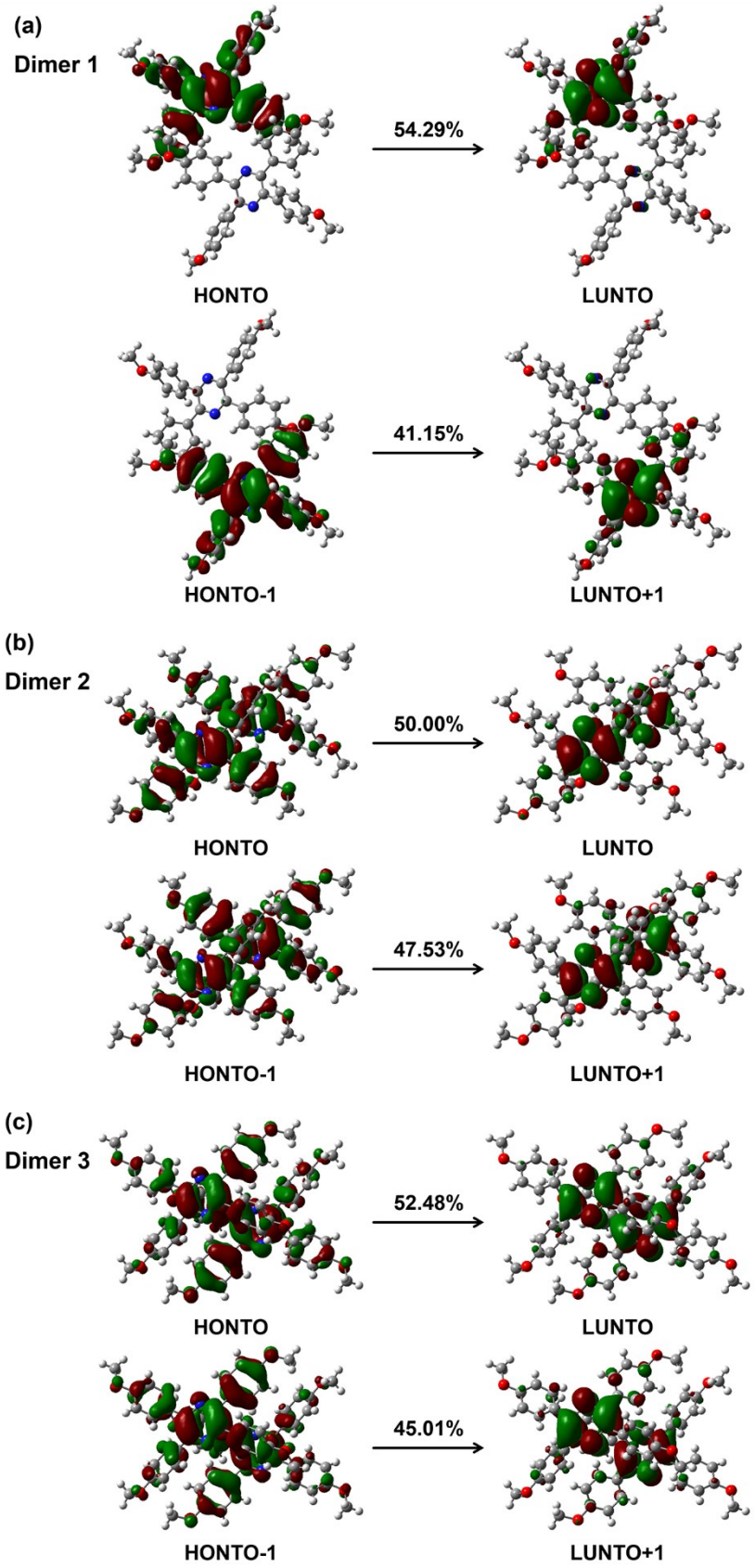

Fig. S2 Transition characteristics and proportions for dimers within ~10 Å of the QM centroid in TPP-4OCH_3 aggregates.

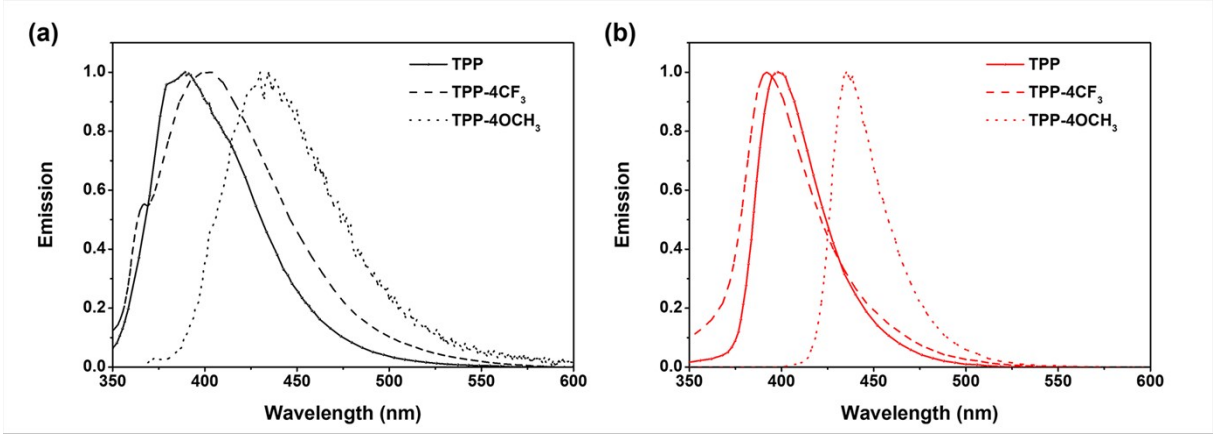

Fig. S3 Normalized PL spectra of TPP and its derivatives in THF solution (10 μM) (a) and crystal (Ex = 310 nm) (b).

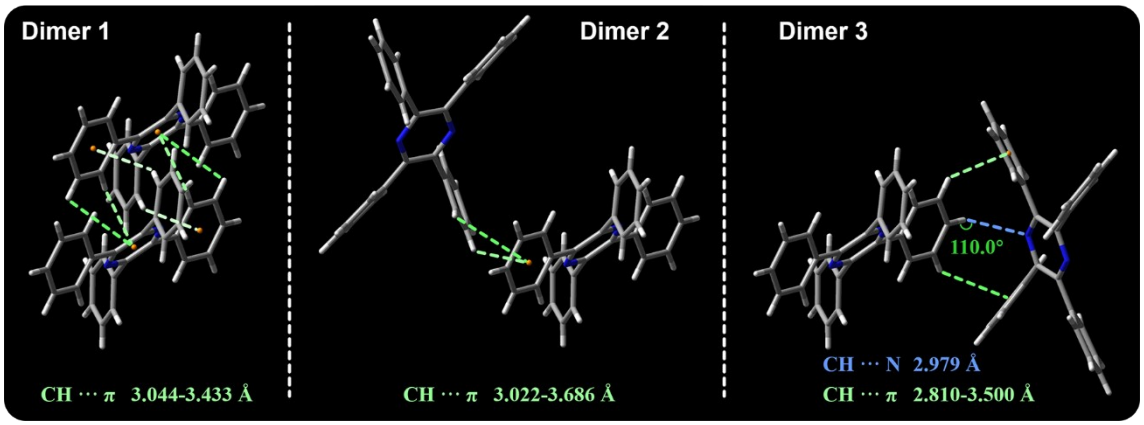

Fig. S4 Relevant intermolecular interactions for dimers of Fig. 2 in TPP aggregates.

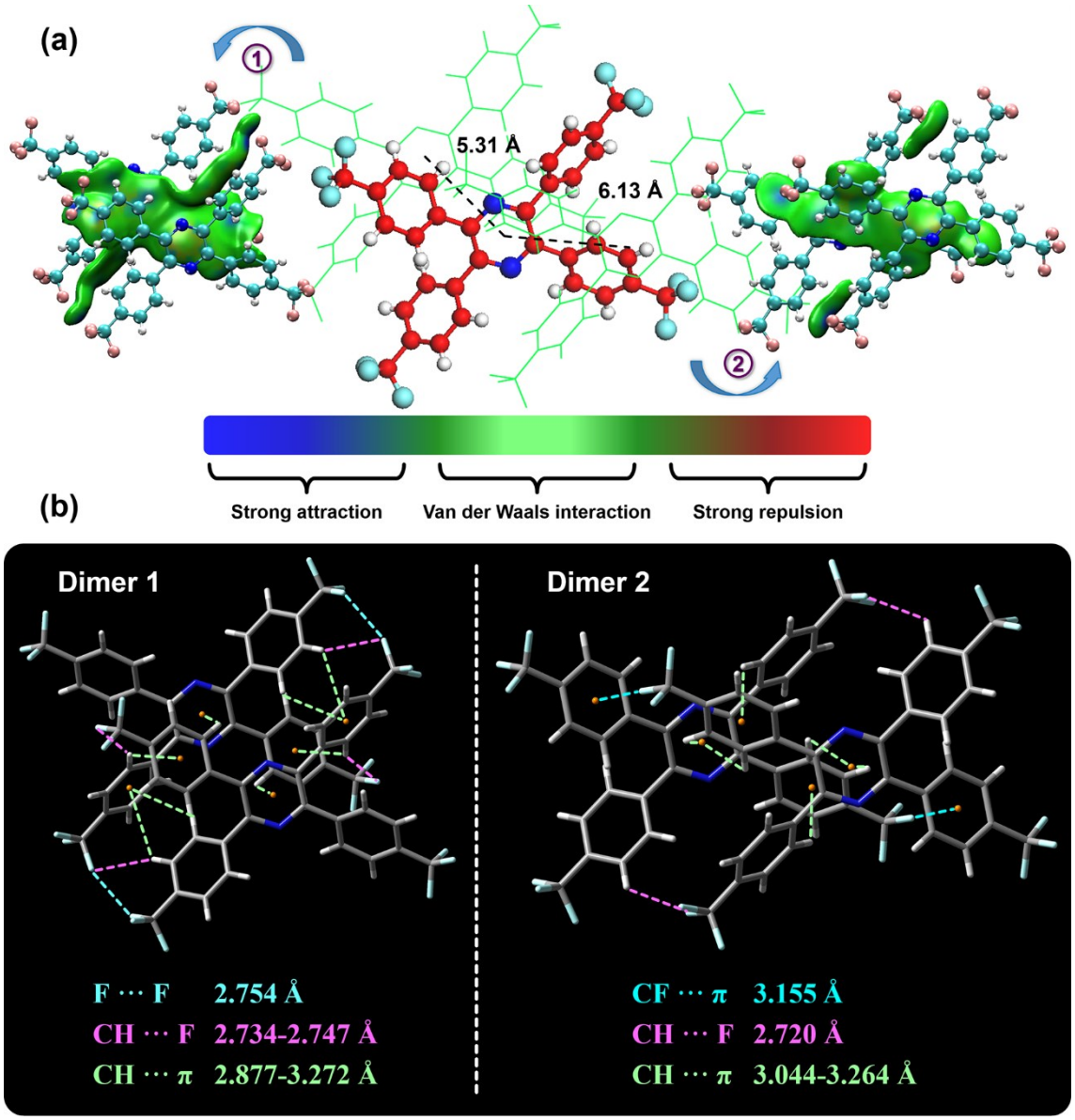

Fig. S5 Molecular packing structures within ~10 Å of the QM centroid (a) and relevant intermolecular interactions (b) in TPP-4CF_3 aggregates.

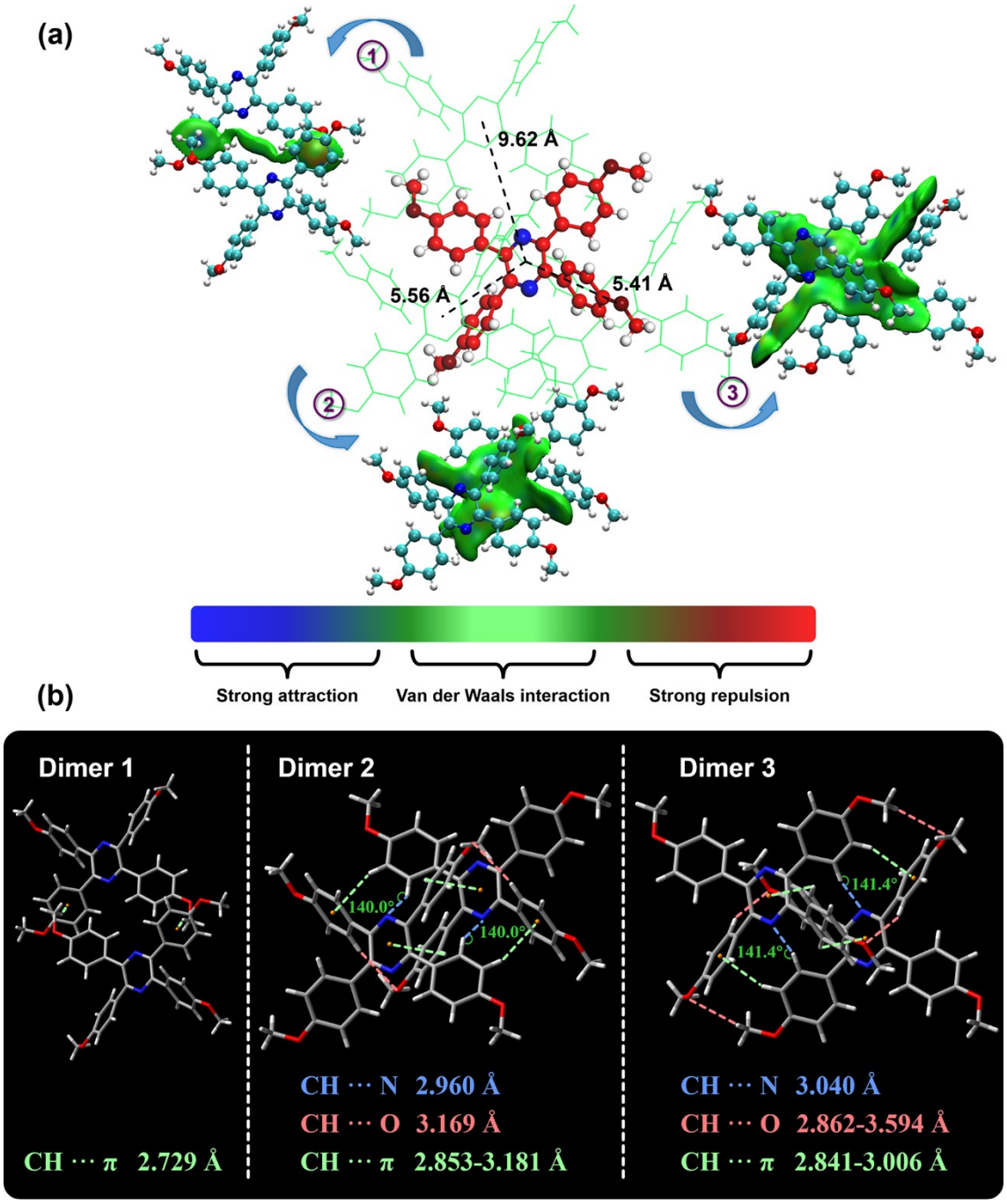

Fig. S6 Molecular packing structures within ~10 Å of the QM centroid (a) and relevant intermolecular interactions (b) in TPP-4OCH$_3$ aggregates.

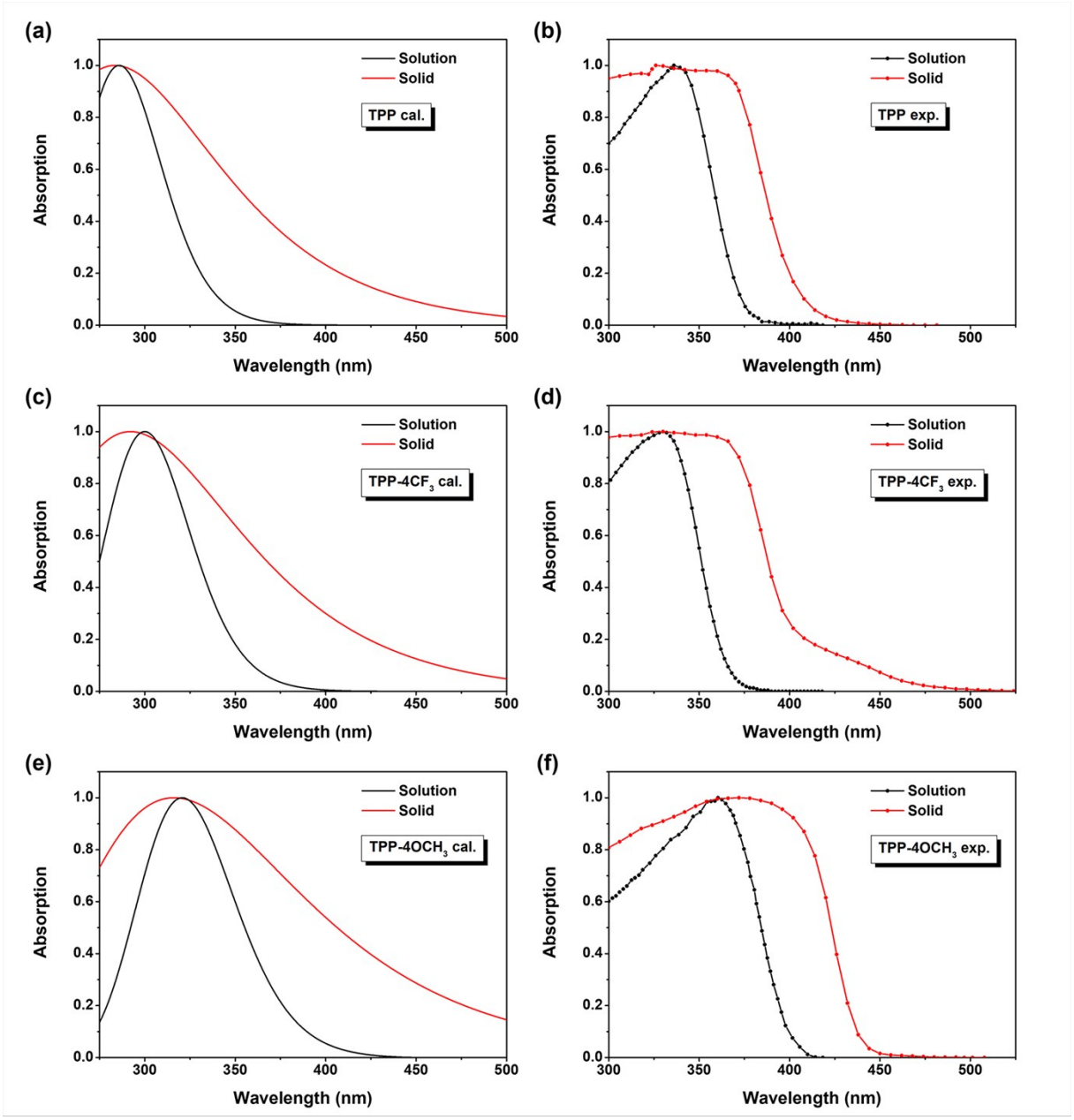

Fig. S7 Calculated (cal., a, c, e) and experimental (exp., b, d, f) UV-Vis absorption spectra for TPP and its derivatives in THF solution and crystal.

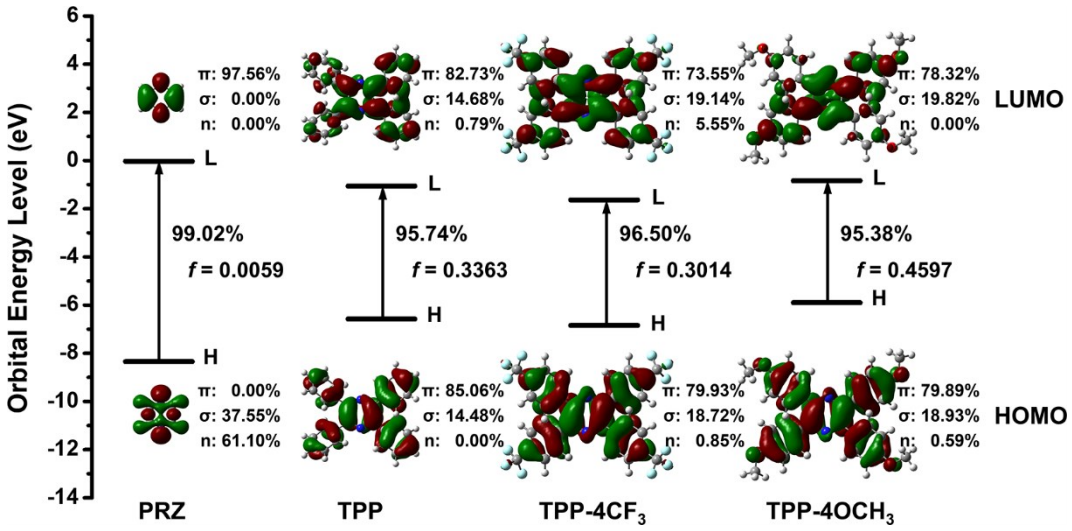

Fig. S8 Involved molecular orbitals in the energy levels, charge density distributions, transition proportions and oscillator strengths for PRZ, TPP and its derivatives at the S_1-optimized geometries in solution.

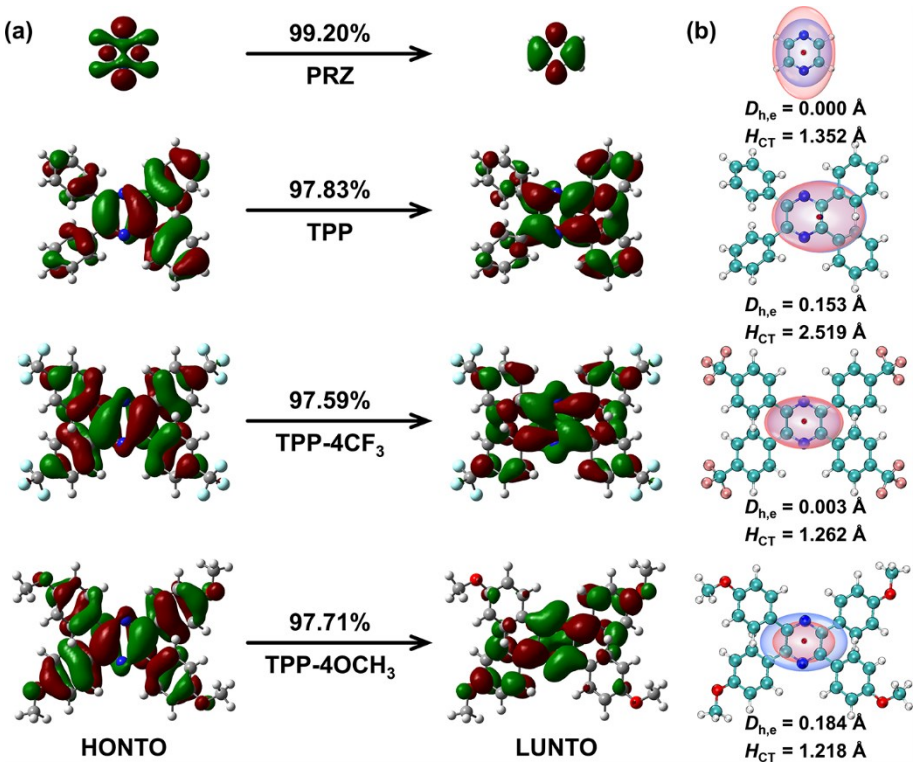

Fig. S9 NTO characters and transition proportions for PRZ, TPP and its derivatives at the S_1-optimized geometries in solution (a). Centroids of holes (red region) and electrons (blue region) of the corresponding transition at the optimized structures, with the labels of holes/electrons centers (red/blue point) and two indexes ($D_{h,e}$ and H_{CT}) (b).

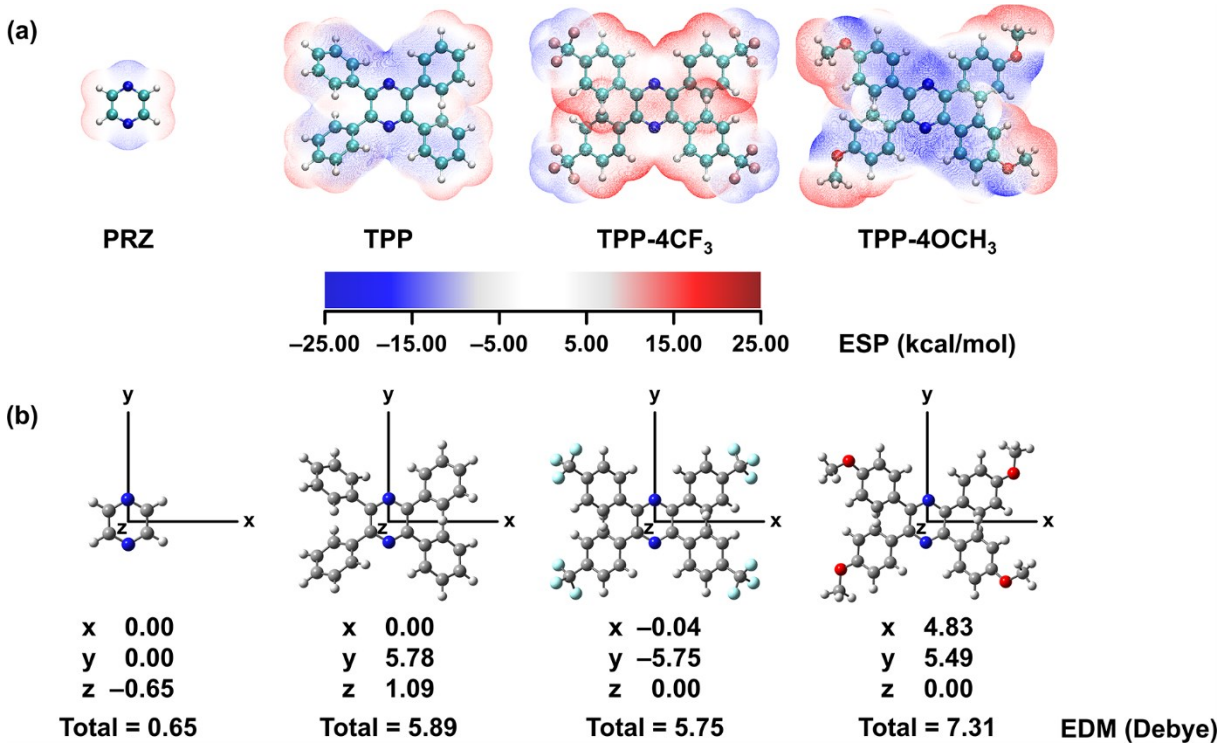

Fig. S10 ESP isosurfaces of electron density (a) and EDM values (b) for PRZ, TPP and its derivatives at the S_1-optimized geometries in solution.

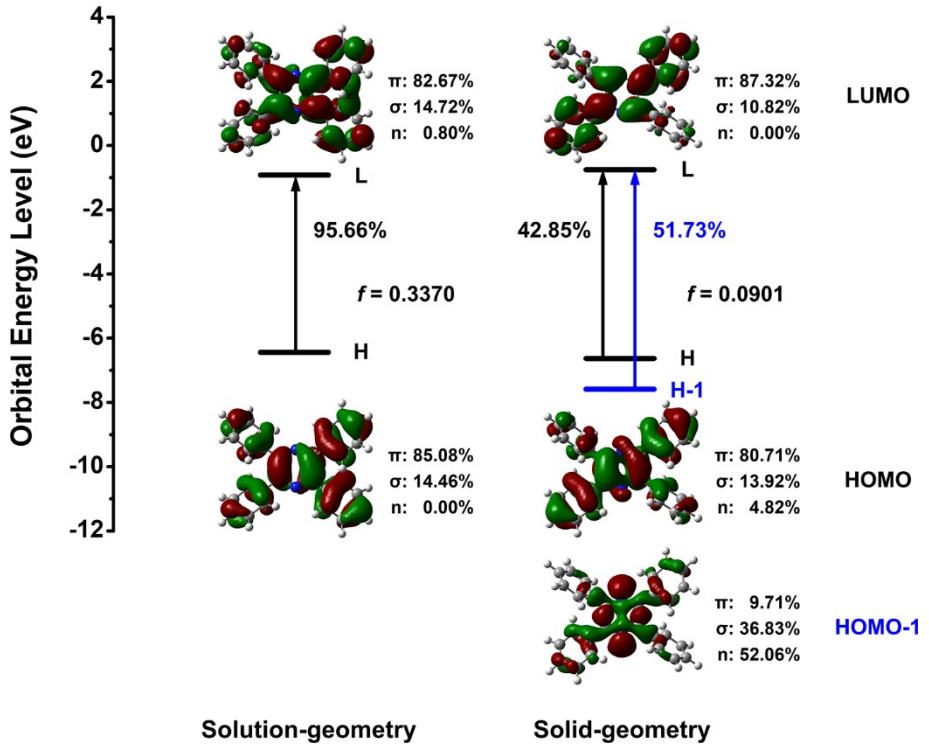

Fig. S11 Gas-phase transition properties for TPP with molecular structure maintaining S_1-optimized geometry in solution and solid, respectively.

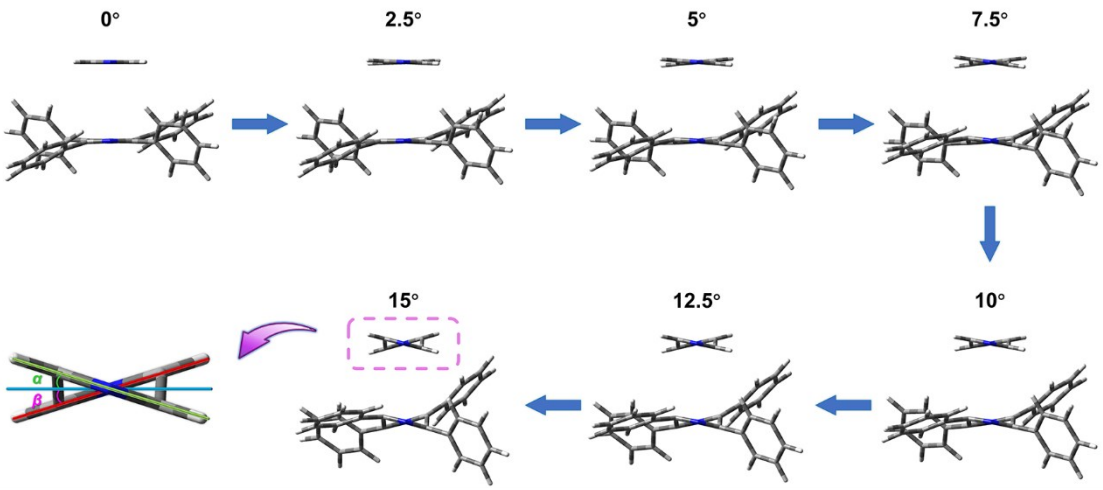

Fig. S12 Demonstration of molecular motion by twisting the pyrazine ring of TPP and individual PRZ alongside the N_1-N_2 linked axis.

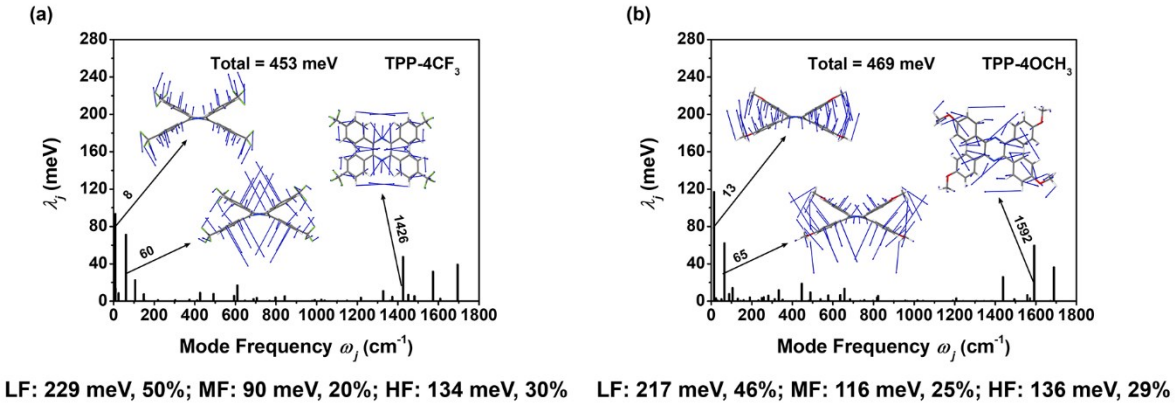

Fig. S13 Relaxation energy λ_j of each normal mode for TPP-$4CF_3$ (a) and TPP-$4OCH_3$ (b) in solution.

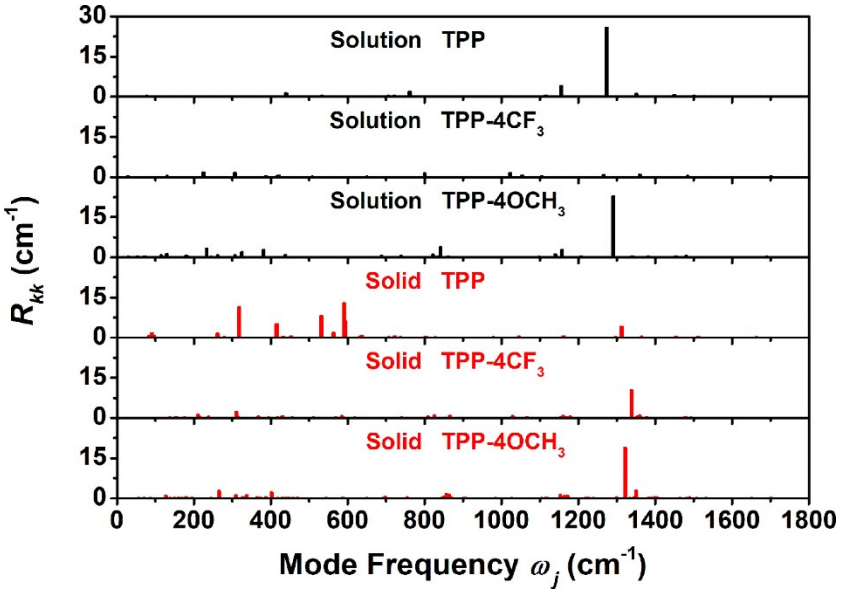

Fig. S14 Diagonal elements R_{kk} of the electronic coupling matrix R_{kl} versus mode frequency ω_j for TPP derivatives in solution (black) and solid (red).

Table S1 Calculated emission wavelengths (in nm) by using different functionals based on the S_1-optimized geometries at the level of PBE0/6-31G(d), as well as the experimental data (exp.) for TPP and its derivatives in solution and solid.

Solution	HF%	TPP	TPP-4CF_3	TPP-4OCH_3
exp.	—	390[a]	400[a]	433[a]
CAM-B3LYP	—	384	417	433
M062X	54	383	414	430
BMK	42	391	421	439
PBE0	25	418	448	472
B3LYP	20	431	461	487
Solid				
exp.	—	398[b]	392[b]	435[b]
CAM-B3LYP	—	392	386	367
M062X	54	402	396	364
BMK	42	409	403	376
PBE0	25	434	429	414
B3LYP	20	445	441	430

[a] In THF solution. [b] In crystal.

Table S2 Selected dihedral angles (in deg) for PRZ in solution and solid. S_0/S_1 and Δ represent the geometric parameters extracted from the optimized S_0/S_1 states and the modifications between the two states, respectively.

		S_0	S_1	Δ	S_0	S_1	Δ
		Solution			Solid		
PRZ	5-	0.07	0.01	0.06	0.14	–0.09	0.23
	6-	–0.07	–0.01	0.06	–0.14	0.10	0.24

Table S3 Calculated configuration proportion α_n% of occupied frontier orbitals for S_1 states based on natural atomic orbital (NAO) method in solid.

PRZ			TPP-4OCH$_3$		
α_n% = 60.70% * 99.06% = 60.13%			α_n% = 0.49% * (90.15% + 4.40%) = 0.46%		
Basis	Atom	α_n^i	Basis	Atom	α_n^i
P_Y	1(N)	30.34%	P_Y	1(N)	0.24%
P_Y	2(N)	30.36%	P_Y	2(N)	0.25%
TPP					
α_n% = 51.81% * 50.90% + 4.57% * 43.58% = 28.36%					
HOMO−1			HOMO		
Basis	Atom	α_n^i	Basis	Atom	α_n^i
P_Y	1(N)	26.87%	P_Y	1(N)	2.34%
P_Y	2(N)	24.94%	P_Y	2(N)	2.23%
TPP-4CF$_3$					
α_n% = 50.63% * 49.07% + 5.42% * 43.52% = 27.20%					
HOMO−1			HOMO		
Basis	Atom	α_n^i	Basis	Atom	α_n^i
P_Y	1(N)	22.81%	P_Y	1(N)	4.91%
P_Y	2(N)	27.82%	P_Y	2(N)	0.52%

Table S4 Calculated configuration proportions α_π%, α_σ% and α_n% of occupied frontier orbitals for S_1 states based on NAO method in solid.

Solid	α_n%	α_σ%	α_π%
PRZ	60.13%	37.56%	0.00%
TPP	28.36%	24.79%	40.37%
TPP-4CF$_3$	27.20%	23.01%	41.49%
TPP-4OCH$_3$	0.46%	13.84%	79.75%

Table S5 Calculated configuration proportion α_n% of occupied frontier orbitals for S_1 states based on NAO method in solution.

PRZ			TPP-4OCH$_3$		
α_n% = 61.10% * 99.02% = 60.49%			α_n% = 0.59% * 95.38% = 0.56%		
Basis	Atom	α_n^i	Basis	Atom	α_n^i
P_Y	1(N)	30.55%	P_Y	1(N)	0.29%
P_Y	2(N)	30.55%	P_Y	2(N)	0.29%
TPP			TPP-4CF$_3$		
α_n% = 0.00% * 95.74% = 0.00%			α_n% = 0.85% * 96.50% = 0.82%		
Basis	Atom	α_n^i	Basis	Atom	α_n^i
P_Y	1(N)	0.00%	P_Y	1(N)	0.42%
P_Y	2(N)	0.00%	P_Y	2(N)	0.42%

Table S6 Calculated configuration proportions α_π%, α_σ% and α_n% of occupied frontier orbitals for S_1 states based on NAO method in solution.

Solution	α_n%	α_σ%	α_π%
PRZ	60.49%	37.18%	0.00%
TPP	0.00%	13.86%	81.44%
TPP-4CF$_3$	0.82%	18.06%	77.13%
TPP-4OCH$_3$	0.56%	18.06%	76.20%

Table S7 Average ESP values (kcal/mol) on the local surface of carbon atoms for PRZ, TPP and its derivatives in solid. The mean values of total carbon atoms in a single ring are given in bold. Average of pyrazine core and four phenyl rings are shown in red and blue, respectively.

Labels	PRZ	TPP	TPP-4CF_3	TPP-4OCH_3
Pyrazine core	**–0.56**	**–5.37**	**11.29**	**–12.28**
C3	–0.74	–5.40	11.67	–12.92
C4	–0.36	–5.14	12.36	–12.61
C5	–0.73	–5.80	9.38	–11.19
C6	–0.42	–5.13	11.75	–12.41
Phenyl rings		**–15.70**	**0.85**	**–17.49**
ring 1		**–15.33**	**1.73**	**–17.51**
C7		–15.84	4.57	–20.61
C8		–16.86	1.45	–19.97
C10		–14.24	0.24	–15.39
C12		–13.40	0.96	–12.42
C14		–15.34	0.50	–17.90
C16		–16.30	2.65	–18.80
ring 2		**–15.61**	**2.05**	**–18.52**
C18		–21.70	0.52	–23.40
C19		–16.30	2.41	–19.81
C21		–13.58	4.21	–16.63
C23		–12.30	3.44	–13.64
C25		–11.82	1.99	–17.17
C27		–17.99	–0.30	–20.48
ring 3		**–15.44**	**–0.14**	**–16.73**
C29		–16.16	–1.46	–21.59
C30		–17.20	0.56	–19.74
C32		–14.72	0.98	–14.18
C34		–13.32	1.05	–10.96
C36		–15.07	–0.35	–15.01
C38		–16.14	–1.63	–18.91
ring 4		**–16.42**	**–0.23**	**–17.21**
C40		–22.11	–2.72	–24.78
C41		–17.38	–0.48	–19.36
C43		–14.64	1.21	–12.38
C45		–12.99	1.56	–9.69
C47		–12.63	–0.12	–16.23
C49		–18.78	–0.82	–20.81

Table S8 Average ESP values (kcal/mol) on the local surface of carbon atoms for PRZ, TPP and its derivatives in solution. The mean values of total carbon atoms in a single ring are given in bold. Average of pyrazine core and four phenyl rings are shown in red and blue, respectively.

Labels	PRZ	TPP	TPP-4CF_3	TPP-4OCH_3
Pyrazine core	**–0.10**	**–5.74**	**13.46**	**–14.78**
C3	–0.07	–5.75	13.48	–14.20
C4	–0.11	–5.71	13.45	–15.33
C5	–0.14	–5.77	13.50	–14.21
C6	–0.08	–5.72	13.41	–15.37
Phenyl rings		**–14.65**	**2.80**	**–17.02**
ring 1		**–13.71**	**2.81**	**–16.00**
C7		–15.60	5.03	–19.53
C8		–14.95	3.25	–17.02
C10		–13.31	1.30	–13.25
C12		–11.87	1.74	–11.34
C14		–12.00	2.50	–16.21
C16		–14.52	3.05	–18.65
ring 2		**–13.69**	**2.80**	**–18.03**
C18		–15.43	5.02	–22.29
C19		–14.61	3.06	–19.05
C21		–11.96	2.46	–14.74
C23		–11.88	1.76	–13.40
C25		–13.32	1.30	–18.52
C27		–14.95	3.23	–20.17
ring 3		**–15.58**	**2.81**	**–16.01**
C29		–19.84	5.02	–19.60
C30		–16.34	3.23	–17.06
C32		–13.98	1.31	–13.22
C34		–13.10	1.79	–11.23
C36		–13.51	2.46	–16.23
C38		–16.71	3.07	–18.74
ring 4		**–15.61**	**2.79**	**–18.04**
C40		–20.05	4.99	–22.28
C41		–16.70	3.05	–19.10
C43		–13.49	2.47	–14.72
C45		–13.07	1.70	–13.40
C47		–13.99	1.32	–18.54
C49		–16.38	3.24	–20.22

Table S9 Rotation magnitude of four phenyls and the configuration proportion α_n% of occupied frontier orbitals for TPP in gas phase.

TPP				
1-	–10.00	–20.00	–30.00	–40.00
2-	–10.00	–20.00	–30.00	–40.00
3-	10.00	20.00	30.00	40.00
4-	10.00	20.00	30.00	40.00
α_n%	4.12%	18.24%	30.78%	35.64%

Table S10 Twisting degree of the pyrazine ring and the configuration proportion α_n% of occupied frontier orbitals for TPP and PRZ in gas phase.

α / β	0°	2.5°	5°	7.5°	10°	12.5°	15°
TPP							
α_n%	29.00%	28.45%	26.10%	22.16%	17.09%	11.86%	7.71%
PRZ							
α_n%	60.51%	60.14%	59.02%	56.70%	53.16%	51.62%	49.00%

Table S11 Relaxation energies (meV) of low-frequency modes (λ_{LF}, <200 cm^{-1}), mid-frequency modes (λ_{MF}, 200–1400 cm^{-1}) and high-frequency modes (λ_{HF}, 1400–1800 cm^{-1}), as well as their contributions to the total λ_{total} for TPP and its derivatives in solution and solid.

Solution	λ_{LF}	λ_{MF}	λ_{HF}	λ_{total}	$\lambda_{LF}/\lambda_{total}$	$\lambda_{MF}/\lambda_{total}$	$\lambda_{HF}/\lambda_{total}$
TPP	319	118	162	599	0.53	0.20	0.27
TPP-4CF_3	229	90	134	453	0.50	0.20	0.30
TPP-4OCH_3	217	116	136	469	0.46	0.25	0.29
Solid							
TPP	95	286	210	591	0.16	0.48	0.36
TPP-4CF_3	50	239	197	486	0.10	0.49	0.41
TPP-4OCH_3	62	111	92	265	0.23	0.42	0.35

Table S12 Relaxation energies (meV) from bond length λ_{bond}, bond angle λ_{angle} and dihedral angle $\lambda_{dihedral}$, as well as their contributions to the total λ_{total} for TPP and its derivatives in solution and solid.

Solution	λ_{bond}	λ_{angle}	$\lambda_{dihedral}$	λ_{total}	$\lambda_{bond}/\lambda_{total}$	$\lambda_{angle}/\lambda_{total}$	$\lambda_{dihedral}/\lambda_{total}$
TPP	221	7	371	599	0.369	0.012	0.619
TPP-4CF_3	206	12	235	453	0.455	0.026	0.519
TPP-4OCH_3	182	18	269	469	0.388	0.038	0.574
Solid							
TPP	187	196	208	591	0.316	0.332	0.352
TPP-4CF_3	184	180	122	486	0.379	0.370	0.251
TPP-4OCH_3	115	55	95	265	0.434	0.208	0.358

Table S13 Bond angles with large relaxation energies (>1 meV) for TPP and its derivatives in solution and solid.

Solution					
TPP	meV	TPP-4CF_3	meV	TPP-4OCH_3	meV
Junction		**Junction**		**Pyrazine core**	
N2-C4-C18	2.46	N1-C3-C7	2.00	C3-N1-C6	3.12
N1-C3-C7	2.46	N2-C5-C29	2.00	C4-N2-C5	3.12
C4-C3-C7	1.26	N2-C4-C18	1.95	**Junction**	
C3-C4-C18	1.26	N1-C6-C40	1.95	N2-C5-C29	2.40
C4-C18-C27	1.19			N1-C3-C7	2.40
C3-C7-C8	1.19			C5-C6-C40	1.69
Phenyl rings				C3-C4-C18	1.69
C19-C18-C27	1.07			**Phenyl rings**	
C8-C7-C16	1.07			C30-C29-C38	1.46
				C8-C7-C16	1.45
Solid					
Pyrazine core		**Pyrazine core**		**Pyrazine core**	
C3-N1-C6	45.63	C3-N1-C6	55.69	N1-C6-C5	11.36
C4-N2-C5	41.74	N1-C3-C4	24.18	C3-N1-C6	11.24
N2-C5-C6	17.79	C4-N2-C5	16.51	C4-N2-C5	8.71
N1-C3-C4	17.13	N2-C5-C6	13.54	N2-C4-C3	7.11
N1-C6-C5	6.88	N1-C6-C5	2.78	**Junction**	
N2-C4-C3	5.77	N2-C4-C3	1.95	C5-C6-C40	3.29
Junction		**Junction**		N1-C6-C40	2.25
N2-C4-C18	15.95	N2-C5-C29	17.32	C3-C4-C18	1.86
N1-C6-C40	13.80	N2-C4-C18	13.56	N2-C4-C18	1.67
N2-C5-C29	8.47	N1-C3-C7	12.71	C3-C7-C16	1.25
N1-C3-C7	7.56	C3-C4-C18	5.72	**Phenyl rings**	
C5-C29-C38	2.74	N1-C6-C40	4.81	C8-C7-C16	1.19
C3-C7-C16	2.72	C3-C7-C16	2.33	C30-C29-C38	1.03
C3-C4-C18	2.35				
Phenyl rings					
C30-C29-C38	1.33				
C8-C7-C16	1.08				

Table S14 N1···N2 distance (in Å) and selected bond angles (in deg) at the optimized S_0 states for TPP and its derivatives. Δ represents the geometric difference between solution and solid.

	Solution	Solid	Δ	Solution	Solid	Δ	Solution	Solid	Δ
	TPP			TPP-4CF_3			TPP-4OCH_3		
B(N1···N2)	2.78	2.63	–0.15	2.77	2.62	–0.15	2.77	2.81	0.04
A(C3-N1-C6)	120.83	128.28	7.45	119.81	129.35	9.54	119.05	117.69	–1.36
A(C4-N2-C5)	120.83	128.05	7.22	119.81	127.65	7.84	119.05	117.61	–1.44